Journal Name

ARTICLE

Multifunctional intercalation in layered double hydroxide: Toward multifunctional nanohybrid for epoxy resin

Received 00th January 20xx,

Accepted 00th January 20xx

DOI: 10.1039/x0xx00000x

www.rsc.org/

Ehsan Naderi Kalali, Xin Wang and De-Yi Wang*

Multifunctional intercalation in layered double hydroxide (LDH) has been developed via designed multi-modifiers with varied functions in order to transfer these functions to epoxy material by nanocarrier. The functions of the multi-modifiers' system include: (i) functionalized hydroxypropyl-sulfobutyl-beta-cyclodextrin (sCD) and phytic acid (Ph) aim at enhancing flame retardancy; (ii) sodium dodecylbenzenesulfonate (SDBS) enlarges the interlayer space of LDHs for facilitating LDH's dispersion in epoxy matrix; (iii) chalcone imparts the anti-UV property to epoxy matrix. In contrast to conventional LDHs based epoxy composites, the functionalized LDH (fLDH) based epoxy nanocomposites show significantly improvement on both flame retardancy, such as passing UL94 V0 rating and reduction of Peak of Heat Release Rate over 70%, and anti-UV properties in terms of well maintenance on impact, flexural and micro-mechanical properties after 100, 200 300, 400h UV irradiation, respectively. Such multifunctional nanohybrid may be used to develop varied functional and sustainable epoxy-based materials for some advanced application.

1. Introduction

Due to the low cost, ease of processing, good adhesive, excellent mechanical properties and solvent resistance, epoxy resins (EPs) have attracted considerable attention over the past few decades.[1-4] EPs have been commonly used as advanced composites matrices in the field of electric/electronic devices where a remarkable flame-retardant grade is required, but its high flammability is a major drawback of these materials. Traditionally, halogenated compounds are widely used as co-monomers or additive with epoxy resins to obtain fire-retardant materials. Despite of high efficiency of halogenated compounds, environmental concerns over the potential risks that halogenated chemicals pose have been a reality for the last decade.[5-7] To overcome this issue, both the academic and industrial communities have been devoted to develop non-halogenated environmentally friendly flame retardant additives.

The rise of nanotechnology provides a brand new methodology for flame retardant polymer materials. The suppression effect of nano-additives on the heat release rate of polymers is very impressive compared to conventional flame retardants. For example, incorporation of clay into polypropylene led to as much as a 70% decrease in the peak of heat release rate (pHRR) observed in the cone calorimeter test[8], just at the loading of 10 wt%. Furthermore, the addition of nano-additives showed improvement on the flame retardancy and mechanical properties simultaneously, whereas most of conventional flame retardants cannot. Among various nano-additives, layered double hydroxide (LDH), as a typically inorganic layered crystalline material, has aroused numerous interests in the field of fabricating polymer nanocomposites.[9, 10] LDH has been regarded as one kind of anionic clay with a general molecular formula of $[M^{2+}_{1-x}M^{3+}_{x}(OH)_2]^{x+}.[(A^{n-})_{x/n}\cdot yH_2O]^{x-}$, where M^{2+}, M^{3+}, and A^{n-} represent divalent metal cations, trivalent metal cations, and interlayer anions, respectively.[11] LDHs could form the intercalated and/or exfoliated structure and thus result in improved mechanical properties, enhanced thermal stability[12] and optical properties.[13] Also, it has been proved that LDHs is a very efficient additive in improving fire retardant performance of polymers.[14, 15] However, although LDHs are very effective in lowering the pHRR of polymers, the most of their composites fail to some special industrial fire measurement, like the UL-94 vertical burning test.[16]

In order to obtain polymer materials with excellent fire resistance for some industrial application, LDHs are combined with phosphorus-containing compounds to create flame retardant synergism. When incorporating LDHs into polymer matrices, they tend to form aggregates due to the strong Van der Waals forces among the inter-layers. Therefore, it is necessary to modify the pristine LDH to enlarge the interlayer distance, to alter the surface properties, and to facilitate dispersion in the polymers.[17] A wide variety of anionic surfactants, such as fatty acid salts[18], sulfonates[19, 20], and phosphates[21], have been utilized to modify LDH. The modified LDHs further enhance the properties of the resultant polymer composites due to the improved dispersion state of the LDHs. Very recently, our group found that by suitable modification for LDH it greatly increased the flame retardant efficiency[9, 10, 22] and improved the mechanical properties.[9] Ideally, the functional LDH is expected to bring some special function to

[a] IMDEA Materials Institute, C/Eric Kandel, 2, 28906 Getafe, Madrid, Spain. E-mail: deyi.wang@imdea.org†

polymers via employing function of modifiers, like flame retardant synergism or other important properties.

One of the popular applications of epoxy composites is for manufacturing electrical appliances as encapsulating materials, and thus the photo-stability and the thermal stability of these encapsulating materials would be of great importance.[23] UV radiation is amongst the most severe weathering conditions that can result in adverse effects on the mechanical properties of the epoxy matrix. UV photons absorbed by epoxy matrix result in photo oxidative reactions that alter the chemical structure resulting in material deterioration.[24] with relatively short periods of exposure, only changes in surface morphology are observed. However, with extended exposure to UV radiation, the ultimate mechanical characteristics, especially stiffness and impact strength of polymers, are very sensitive to irradiation which can eventually lead to complete disintegration of the material.[25, 26] Therefore, to improve the anti-UV properties for epoxy-based materials is very important.

In this context, aiming to develop high performance epoxy materials with both flame retardancy and anti-UV properties, in this report multifunctional intercalation in LDH by designing multi-modifiers' system instead of individual modifier is proposed to prepare multifunctional LDH (fLDH). Then, cured epoxy/fLDH nanocomposites are prepared by classic epoxy curing procedure. The multi-modifier system was composed of bio-based phytic acid (Ph), functional cyclodexrin (sCD) inserted by Chalcone species, and sodium dodecylbenzenesulfonate (SDBS). In this multi-modifier system, phytic acid acts as an acid source in the condensed phase due to the abundant phosphorus element in its structure; chalcone species serve as anti UV agent; sCD can function as a char agent during the combustion due to a large number of hydroxyl groups in its structure; and SDBS is used to enlarge the interlayer gallery distance of the LDH layers and thus to improve the dispersion state of the LDH layers. Varied functional LDHs were synthesized by one-step method and characterized by X-ray diffraction (XRD). The morphology of the resultant modified LDH based epoxy nanocomposites was investigated by XRD and transmission electron microscopy (TEM). The fire retardant behavior of LDH based epoxy nanocomposites were characterized by limited oxygen index (LOI), vertical burning test (UL-94), and cone calorimeter tests (CCT). Anti-UV properties are studied in term of the change of impact, flexural and micro-mechanical properties against the UV irradiation for 0, 100, 200, 300, 400h, respectively.

2. Experimental

2.1. Materials

Magnesium nitrate hexahydrate, aluminum nitrate nonahydrate, sodium hydroxide, sodium dodecylbenzenesulfonate (SDBS), phytic acid sodium salt, β-cyclodextrin, 1, 4-butane sultone (BS) and chalcone were supplied by Sigma-Aldrich and used without further purification. Epoxy resin (Epoxydhedraz C) was supplied by R&G Faserverbundwerkstoffe GmbH- Germany. Diamino diphenyl sulfone (DDS) was provided by TCI Chemicals Company. Spectra/Por®6 dialysis membrane with MWCO-1000 was provided from Carl Roth GmbH & Co. KG, Karlsruhe, Germany.

2.2. Synthesis of hydroxypropyl-sulfobutyl-beta-cyclodextrin (sCD)[28]

In a three-neck round flask equipped with iso-barically funnel, reflux-condenser, and thermometer, β-cyclodextrin (0.02 mol), sodium hydroxide (0.11 mol) and de-ionized water (45 ml) were introduced and stirred until complete dissolution. The solution was heated to 75 °C, and then 1, 4-butane sultone (0.08 mol) was added dropwise within 3 hours. The solution kept stirring for another 4 hours and then cooled down to the room temperature. The above solution was neutralalized with hydrochloric acid and by-products were removed by filtrate dialysis. After filtrate dialysis, the white crystal-like solid product (sCD) was obtained using rotary evaporation method. The chemical formula of sCD could be represented by $C_{42}H_{70}O_{35}\cdot(C_4H_8O_3S)_x$, where X is the substitution number of 1,4-butane sultone. On the basis of NMR (^{1}H-NMR, 500 MHz, DMSO, d, ppm): 4.82 (m, 2H), 1.63-2.21 (m, 4H) and elemental analysis data (N: 1.37%, C: 35.5%, S: 9.15% and H: 7.27%), the degree of substitution of 1,4-butane sultone was approximately 6, which means 6 sulfobutyl groups were covalently attached to cyclodextrin.[9]

2.3. Preparation of functionalized sCD (fCD)

In a three-neck round flask equipped with iso-barically funnel, reflux-condenser, and thermometer, sCD (0.02 mol) and de-ionized water (45 ml) were introduced and stirred until complete dissolution. The solution was heated to 40 °C, and then pre-heated chalcone solution (40 °C, 0.02 mol) was added dropwise within 3 hours. The solution exposed to the ultra-sonication for 5 minutes and then kept stirring for another 24 hours and then cooled down to the room temperature. The greenish yellow crystal-like solid product (fCD) was obtained using rotary evaporation method.

2.4. Synthesis of multifunctional LDHs by one-step method

Following our developed one-step method,[29] in a 1000 ml three-neck round flask equipped with iso-barically funnel, reflux-condenser and pH meter, phytic acid sodium salt (0.03 mol), SDBS (0.04 mol), fCD (0.03 mol) and de-ionized water (300 ml) were charged and stirred until completely dissolved. The nitrate solution containing $Mg(NO_3)_2\cdot 6H2O$ (0.2 mol) and $Al(NO_3)_3\cdot 9H2O$ (0.1 mol) in 300 ml de-ionized water, was then slowly added to the above mixture with vigorous stirring at a constant pH = 10.0 ± 0.5, adjusted by simultaneous drop-wise addition of 1 M NaOH solution. The obtained slurry was continuously stirred for 30 min; afterward, it was allowed to age at 75 °C for 18 h. Finally, the resulting product was filtered and washed thoroughly with de-ionized water until the pH = 7, and then dried at 80 °C until a constant weight which was called fCD-DBS-Ph-LDH. In addition, unmodified LDH (NO_3-LDH), phytic acid sodium salt modified LDH (Ph-LDH), sCD-Ph-LDH

Journal Name

ARTICLE

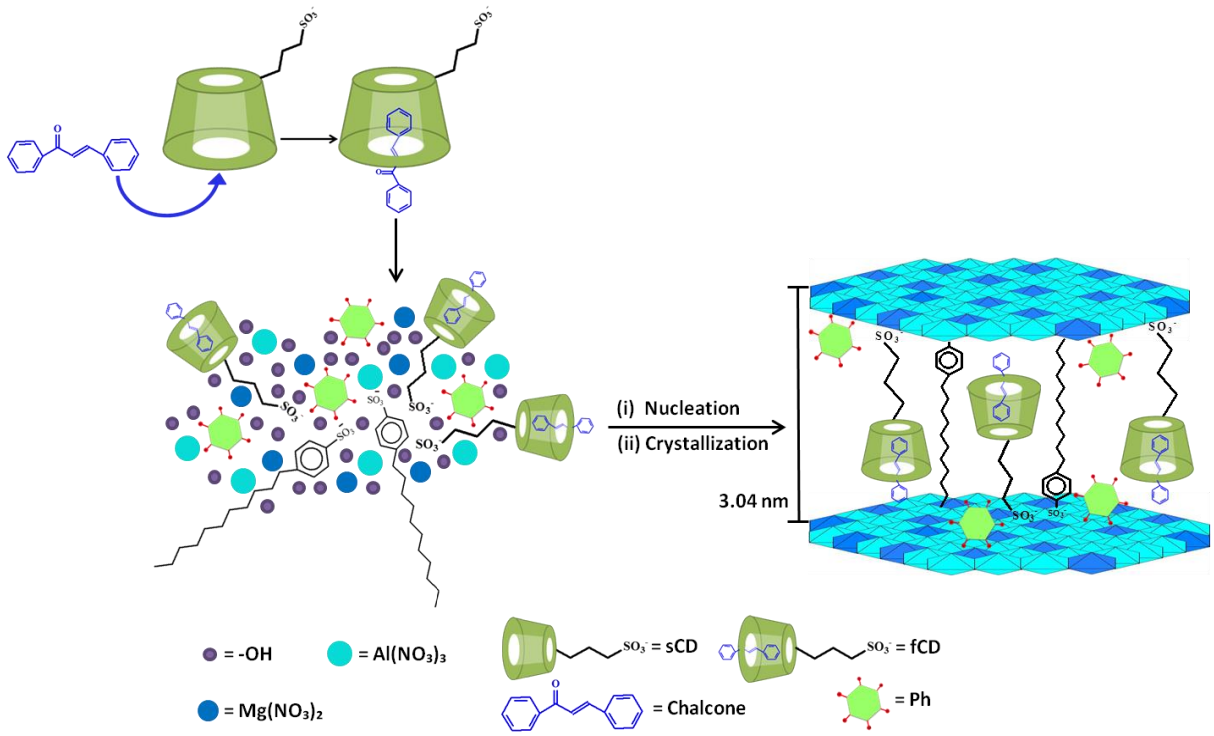

Scheme 1. Schematic diagram of anions structure and intercalated functionalized LDHs (fCD-Ph-DBS-LDH) by one-step synthesis method.

and sCD-DBS-Ph-LDH were synthesized using the similar method. The preparation procedures are shown in Scheme 1.

2.5. Preparation of LDH/epoxy nanocomposites

A fixed weight fraction (7 wt%) of unmodified LDH (NO_3-LDH) or functionalized LDH (Ph-LDH, sCD-Ph-LDH, CD-DBS-Ph-LDH and fCD-DBS-Ph-LDH) was used for the preparation of LDH/epoxy nanocomposites. In order to achieve a satisfactory dispersion state, two-step mixing method was applied. At first, LDH or modified LDH was incorporated into the epoxy matrix using a refined three-roll mill (EXAKT 80E, Germany) for 30 min. In the next step, the mixture was diluted in acetone and exposed to ultra-sonication for 20 min at 60 °C, and then acetone was removed by increasing the temperature gradually until 110 °C and then kept for degassing under the vacuuming to obtain a bubbles-less and viscous mixture. Subsequently, the mixture was heated up to 120 °C and DDS added to the above mixture and stirred for 15 min until DDS totally dissolved. In order to further degassing, the mixture was placed into the vacuum oven at 120 °C for 5 minutes and then immediately poured into the pre-heated PTFE moulds. The curing procedure was set as 150 °C for 1 h, 180 °C for 2 h and 200 °C for 2 h. Following this procedure, NO_3-LDH/EP, Ph-LDH/EP, sCD-Ph-LDH/EP, sCD-DBS-Ph-LDH/EP and fCD-DBS-Ph-LDH/EP were prepared, respectively.

2.6. Characterization

The chemical structure of the prepared samples was identified by FTIR which were recorded on a Thermo Scientific Nicolet IS50 FT-IR spectrometer.

The WAXS patterns of the samples were recorded by a XPERT-PRO X-ray diffractometer. The Cu K_α ($\lambda = 0.1542$ nm) radiation source was operated at 45 kV and 40 mA with a scan speed of 2° min^{-1}.

The surface and cross-section of char residues after cone calorimeter were observed using a Zeiss, EVO MA15 (Germany) scanning electron microscopy.

The morphology and microstructures of the nanocomposites were observed on a Tecnai T20 transmission electron microscopy (TEM) (FEI Company). The accelerated voltage was 200 kV and in order to obtain more clear images, contrasting agent was applied to the samples.

The LOI values were carried out using an Oxygen Index instrument (Fire Testing Technology, UK) according to ASTM D 2863-97. The sample dimensions were 130 × 6.5 × 3.2 mm^3; vertical burning test was carried out by a burning chamber (UL-

94, Fire Testing Technology, UK) with the sample dimension of 127 × 12.7 × 3.3 (±0.2) mm^3 according to ASTM D 3801 standard.

The cone calorimeter tests were carried out on a FTT cone calorimeter, following the procedures in ISO 5660-1. Squared specimens (100 mm × 100 mm × 4 mm) were horizontally irradiated at a heat flux of 50 kW m^{-2}.

Thermogravimetric analysis (TGA) was carried out using a Q50 (TA Instruments) thermo-analyzer instrument at a linear heating rate of 10 °C/min under a nitrogen flow and the samples were dried at 160 °C in the vacuum oven overnight prior to the measurement. The theoretical TG curve was computed by linear combination between the TG curves of neat EP and LDHs. The formula is as follows:

$$W_{th}(T)_{LDH/EP} = x \times W_{exp}(T)_{EP} + y \times W_{exp}(T)_{LDH}, x + y = 1$$

where, $W_{exp}(T)_{EP}$: experimental TG curve of the pure EP; $W_{exp}(T)_{LDH}$: experimental TG curve of LDH; x and y are the weight percentages of the EP and LDH in the composites, respectively.

Three point flexural tests were conducted at cross head speed of 0.5 mm min^{-1} by an Instron 5966 universal bending testing machine. The samples used were rectangular shape with dimensions of 50 mm × 6 mm × 5 mm according to ASTM D-790 standard.

The Charpy impact tests of the un-notched specimens were conducted on a Zorn Standal Instrumented Impact Tester (Germany) at an impact speed of 2.93 m/s. The geometry of the samples was rectangular with dimensions of 50 mm × 6 mm × 4 mm, according to the DIN 53753 standard.

UV radiation was performed in a Solarbox 3000e, equipped with a Xenon lamp with 550 W/m^2 irradiance at 60 °C for 0, 100, 200, 300, 400h, respectively.

Micro Indentation tests were conducted by a Zwick Roell type BZ2.5/TS1S indenter with loading of 5N.

3. Results and discussion

3.1. Characterization of functionalized sCD (fCD)

Fig. 1 shows the X-ray powder diffraction patterns of sCD, chalcone and sCD-chalcone complex. As can be seen, sharp peaks at the diffraction angles of 10, 16, 20 and 22 degree are presented in the diffraction pattern of chalcone. The diffractogram of sCD exhibits some low intensity peaks at particular diffraction angles. In contrast, it is invisible to observe the characteristic peaks of chalcone in the diffraction pattern of sCD-chalcone complex. The substantial decrease in crystallinity of sCD-chalcone complex in comparison with chalcone and the appearance of amorphous corona indicates the incorporation of "guest" molecule (chalcone) into the inner hollow cavity of the "host" compound (sCD) (as shown in inset Fig. 1). In order to further prove the incorporation of the chalcone species into the cavity of sCD, FTIR spectra of sCD, chalcone, their physical mixture and the complex have been recorded, as shown in Fig. S1 in the Supporting Information.

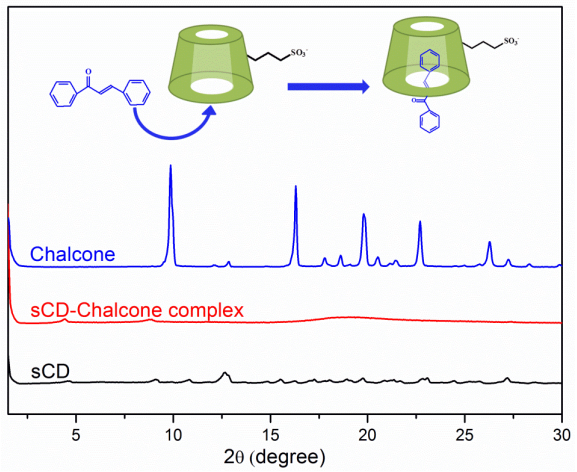

Fig. 1 WAXS patterns of sCD, chalcone and sCD-chalcone complex

3.2. Characterization of functionalized LDH

The WAXS patterns of NO_3-LDH, and modified LDHs are shown in Fig. 2. In the WAXS pattern of NO_3-LDH, the first basal reflection (003) peak appears at 2θ = 9.89° corresponding to an interlayer distance of 0.89 nm. For Ph-LDH, the (003) reflection shifts to 2θ = 7.30° corresponding to the interlayer distance of 1.13 nm. The co-addition of phytic acid and sCD-chalcone complex provided further increase to the interlayer distance of LDH to 2.37 nm. In the case of sCD-DBS-Ph-LDH and fCD-DBS-Ph-LDH the (003) reflection shifts to a lower reflection angle corresponding to an interlayer distance of 3.02 nm and 3.04 nm, which is about 3.5-fold increase in the interlayer distance compared to that of NO_3-LDH. The enlargement of the interlayer distance is caused by the relatively long molecular chains of the sCD/fCD and DBS. DBS is possessing relatively larger molecular size (more than 2 nm) compared to the size of NO_3^- (around 0.1 nm).[9] These results demonstrate that multi-modifier system is effective in enlarging the interlayer distance of LDHs.

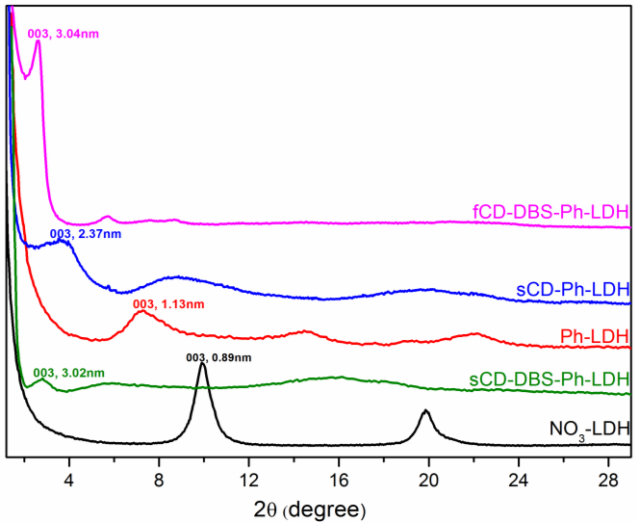

Fig. 2 WAXS patterns of NO_3-LDH, Ph-LDH, sCD-Ph-LDH, sCD-DBS-Ph-LDH and fCD-DBS-Ph-LDH

3.3. Structural characterization of LDH/EP nanocomposites

Usually, the structural morphology of layered nano-filler/polymer nanocomposite was characterized by X-ray scattering patterns in order to determine the microstructures. Fig. 3 shows the WAXS patterns of pure epoxy matrix, NO_3-LDH/EP, sCD-Ph-LDH/EP, sCD-DBS-Ph-LDH/EP and fCD-DBS-Ph-LDH/EP composites. Pure EP had a broad and weak diffraction peak at a 2θ value of 17.3°, due to the amorphous phase of epoxy. NO_3-LDH/EP composite reflected an intense basal diffraction peak at a 2θ value of 9.96° corresponding to an inter-gallery spacing of 0.89 nm, indicating the presence of the ordered structure of unmodified LDH in the polymer matrix. For sCD-Ph-LDH/EP composite, a weak diffraction peak at a 2θ = 3.9° was observed corresponding to an inter-gallery spacing of 2.26 nm, suggesting the swelling of LDH platelets upon polymerization.[9] In the case of sCD-DBS-Ph-LDH/EP and fCD-DBS-Ph-LDH/EP composites, no visible reflection peaks were observed below 10°, indicating highly exfoliated and/or well intercalated LDH platelets within the epoxy resin. Furthermore, this conjecture has been confirmed by TEM and TED.

3.4. Transmission electron microscopy (TEM)

The microstructures of the nanocomposites were characterized by means of transmission electron microscopy (TEM) employed to provide more information in order to investigate the results obtained from the WAXS analysis as well as to directly observe the dispersion state of LDH within the epoxy matrix, as shown in Fig. 4. Low and high magnification TEM images of NO_3-LDH/EP composite (Fig. 4a, b and c) showed that large agglomerations of NO_3-LDHs with the average size of >500 nm were formed. This is the reason why the (003) reflection is observed in the WAXS patterns of NO_3-LDH/EP. The dispersion state of NO_3-LDH/EP was quite different from

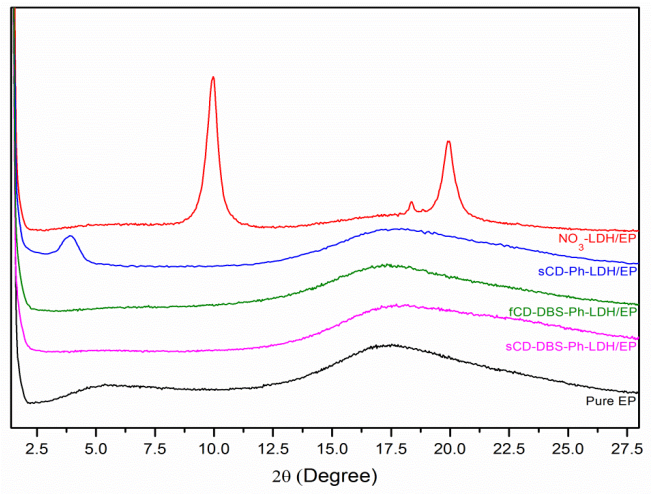

Fig. 3 WAXS patterns of pure EP, NO_3-LDH/EP, sCD-Ph-LDH/EP, sCD-DBS-Ph-LDH/EP and fCD-DBS-Ph-LDH/EP composites

that of fCD-DBS-Ph-LDH/EP. The low and medium magnification TEM image of fCD-DBS-Ph-LDH/EP (Fig. 4d and e) revealed much better dispersion of LDH in the epoxy matrix and the higher magnification image of fCD-DBS-Ph-LDH/EP (Fig. 4f) showed a homogeneously disordered nanostructure, which is in agreement with the WAXS observations. Transmission electron diffraction (TED) patterns were also utilized by TEM in order to investigate the crystalline parameters structures of the specimens. In composite, selected area electron diffraction (SAED) patterns of the NO_3-LDH/EP indicated a clear corona around the pointer (Fig. 4 c), implying the existence of large poly-crystalline structures. In

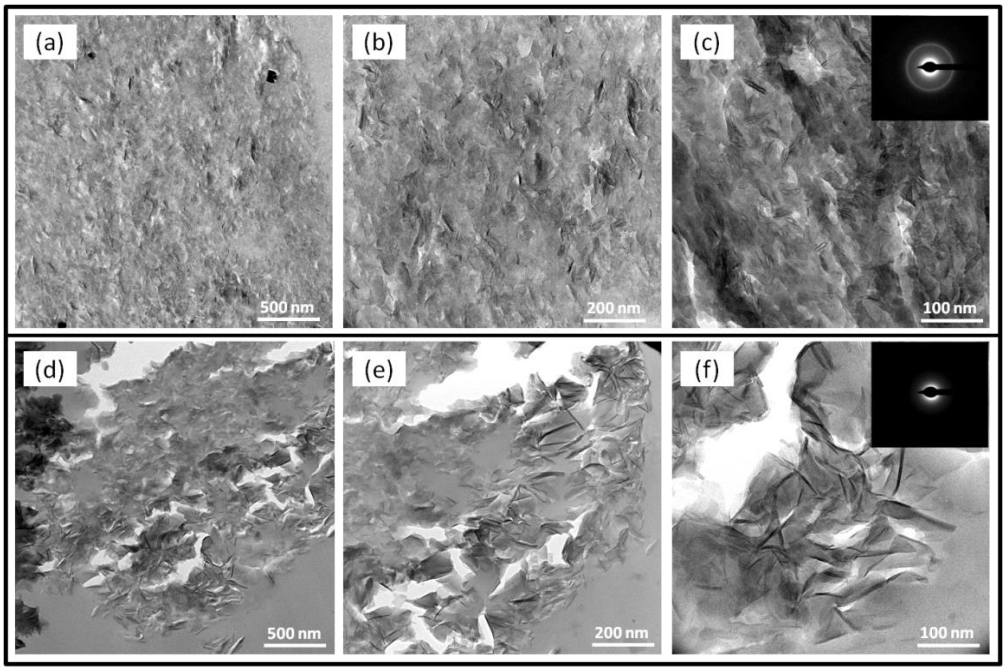

Fig. 4 TEM images of NO_3-LDH/EP (a, b and c) and fCD-DBS-Ph-LDH/EP (d, e and f) nanocomposites.

Journal Name

ARTICLE

contrast, in the SAED image of fCD-DBS-Ph-LDH/EP (Fig. 4f), there was no corona observed around the pointer, which indicated the existence of scant crystallites or excellent exfoliated nano-particles.

3.5. Thermal stability of epoxy nanocomposites

TGA thermograms of un-modified LDH, modified LDHs, pure epoxy and epoxy nanocomposites with various contents are showed in Fig. 5 and the detailed results were summarized in Table 1. Initial degradation temperature ($T_{5\%}$) of functionalized LDH indicated lower value compared with that of unmodified LDH, which was caused by the introduction of thermally instable organic modifiers into LDHs. In case of pure EP it is observed that the main degradation stage ranging from 380 to 500 °C that was attributed to the decomposition of three dimensional macromolecular networks of the matrix. All the LDH-based epoxy nanocomposites exhibited one-stage degradation process similar to pure EP.

However, the $T_{5\%}$ of all the LDH-based epoxy nanocomposites were descended compared to that of pure EP, as a result of the earlier initial decomposition leading by the addition of LDHs. Earlier initial decomposition requisite to form a char layer and hence, protect underneath polymer matrix against flame. It was observed that the char yield at 750 °C was increased due to the incorporation of the functionalized LDHs. In case of pure EP, it produced 14.5% residue at 750 °C, whereas NO_3-LDH/EP, sCD-Ph-LDH/EP, sCD-DBS-Ph-LDH/EP and fCD-DBS-Ph-LDH/EP nanocomposites had 13.6%, 14.9%, 18.2% and 19.5% residues, respectively, at 750 °C. The experimental char yields of sCD-Ph-LDH/EP, sCD-DBS-P-LDH/EP and fCD-DBS-P-LDH/EP were higher than the calculated ones, suggesting that fCD and DBS are good charring agents in combination with phytic acid.

Table 1 TGA results of LDH, organo-modified LDHs and their epoxy nanocomposites

Sample	$T_{5\%}$ (°C)	T_{max} (°C)	Residue yield at 750°C (wt %)	
			Calculated	Experimental
NO_3-LDH	305	395	--	53.8
Ph-LDH	233	340	--	51.5
sCD-Ph -LDH	290	339	--	52.2
sCD-DBS-Ph-LDH	224	467	--	49.8
fCD-DBS-Ph-LDH	223	462	--	43.4
EP	384	413	--	14.5
Ph-LDH/EP	379	407	17.0	18.3
NO_3-LDH/EP	372	407	17.2	10.1
sCD-Ph-LDH/EP	374	406	17.1	19.2
sCD-DBS-Ph-LDH/EP	361	398	16.9	18.7
fCD-DBS-Ph-LDH/EP	363	399	16.5	19.6

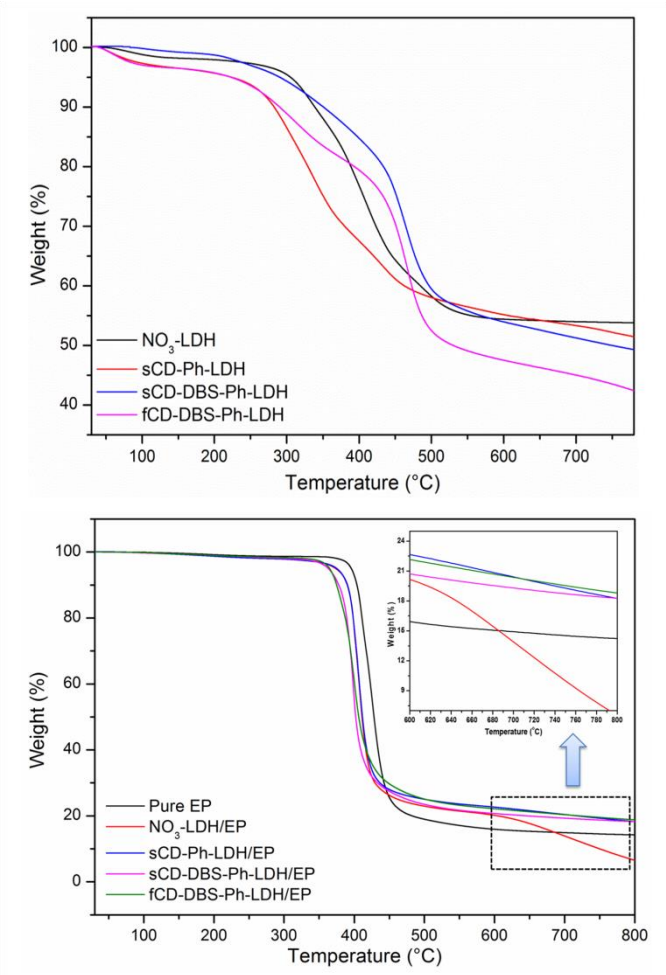

Fig. 5 TGA of NO_3-LDH, sCD-Ph-LDH, sCD-DBS-Ph-LDH, fCD-DBS-Ph-LDH, pure EP and epoxy composites under N_2 at heating rate of 10°C/min.

3.6. Burning behaviour

First of all, the flammability of the cured EP and epoxy nanocomposites were examined by measuring their oxygen index (LOI) and vertical burning test (UL-94) and the final results are summarized in Table 2. Pure epoxy showed a LOI value of 23.0% and no classification in the UL-94 vertical burning test. By adding NO_3-LDH, the LOI value increased to 25.2%, but still indicated no rating in the UL-94 test. Incorporating Ph-LDH and sCD-Ph-LDH improved the LOI value slightly, but both of them still cannot pass the UL-94 V0 rating. However, it was noted that adding sCD-DBS-Ph-LDH

or fCD-DBS-Ph-LDH into epoxy provided a great improvement in LOI,

Table 2 LOI and UL-94 data of pure EP and LDH based Epoxy nanocomposites

Sample	LOI (%)	UL-94	Observation
Pure EP	23.0	No rating	Fire with a sooty flame
NO_3- LDH/EP	26.2	No rating	Fire with a sooty flame
Ph-LDH/EP	23.7	No rating	Fire with a sooty flame
sCD-Ph-LDH/EP	26.5	No rating	Fire with a sooty flame
sCD-DBS-Ph-LDH/EP	26.0	V-0	Extinguished immediately
fCD-DBS-Ph-LDH/EP	26.5	V-0	Extinguished immediately

26 and 26.5 respectively and the UL-94 V0 rating was achieved in vertical burning test.

Measurements in Cone calorimeter have been widely used to detect the combustion characteristics of the polymeric materials. Fig. 6 showed the heat release rate (HRR), total heat release (THR) and smoke temperature versus time curves of pure EP and its nanocomposites. Other various important parameters obtained from the cone calorimeter tests, such as the time-to-ignition (TTI), peak heat release rate (pHRR), total smoke production (TSP), average HRR (Ave. HRR) and the char residue, are summarized in Table 3. Compared with pure EP, NO_3-LDH/EP, sCD-Ph-LDH/EP and sCD-DBS-Ph-LDH/EP composite, the peak of HRR decreased from 835 kW/m^2 to 679 kW/m^2 (-19%), 766 kW/m^2 (-8%) and 349 kW/m^2 (-58%), respectively. In the case of fCD-DBS-Ph-LDH/EP composites, from Fig. 6a, it can be observed that fCD-DBS-Ph-LDH/EP ignited rapidly due to the early initial degradation stage after ignition. The peak HRR of fCD-DBS-Ph-LDH/EP dramatically decreased to 232 kW/m^2, corresponding to a 72% reduction compared to that of pure epoxy. Similar trend was observed for the average HRR values of the pure EP and epoxy nanocomposites which are listed in the Table 3. Pure EP showed the Ave. HRR value of 330 kW/m^2, the NO_3-LDH/EP, sCD-Ph-LDH/EP and sCD-DBS-Ph-LDH/EP indicated 360 kW/m^2, 256 kW/m^2 and 234 kW/m^2 respectively, while fCD-SDBS-Ph-LDH/EP nanocomposite showed 162 kW/m^2 corresponding to a 50% reduction in the Ave. HRR. The good dispersion state of the LDH layers into the epoxy matrix was due to enlarged inter-layer distance of fCD-SDBS-Ph-LDH and improved char yield of epoxy nanocomposites during combustion due to existence of fCD and Ph species are the major aspects of the improved fire retardancy of fCD-DBS-Ph-LDH.

Fig. 6b showed the total heat release rate of the Pure EP and epoxy nanocomposites. At 350 second after the ignition, pure EP released a total heat of 96.7 MJ/m^2, the NO_3-LDH/EP, sCD-Ph-LDH/EP and sCD-DBS-Ph-LDH/EP released 87.8 MJ/m^2, 76.6 MJ/m^2 and 66.4 MJ/m^2 respectively, whereas fCD-SDBS-Ph-LDH/EP nanocomposite only released total heat of 47.2 MJ/m^2. Participation of the organic species in the carbonization process and their presence in the condensed phase instead of going into the gas phase as "fuel" is the main reason of significant reduction of THR in the epoxy resin. This was also can be proved by the increased char residues (as listed in Table 3).

With regard to the smoke temperature (as shown in Fig. 6c), pure EP also displayed the highest smoke temperature among all the samples. The addition of fCD-SDBS-Ph-LDH/EP resulted in relatively decreased smoke temperature compared to pure EP. The decreased smoke temperature in epoxy nanocomposite was probably due to the reduced heat release of epoxy converted into organic volatiles, as the organic volatiles were the major source of heat [9]. According to the TSP values (as listed in Table 3), pure EP shows the highest value among all the samples. In the case of the fCD-SDBS-Ph-LDH/EP nanocomposites, lower TSP (63.5% reduction) was observed compared to pure EP. The decrease in smoke formation in

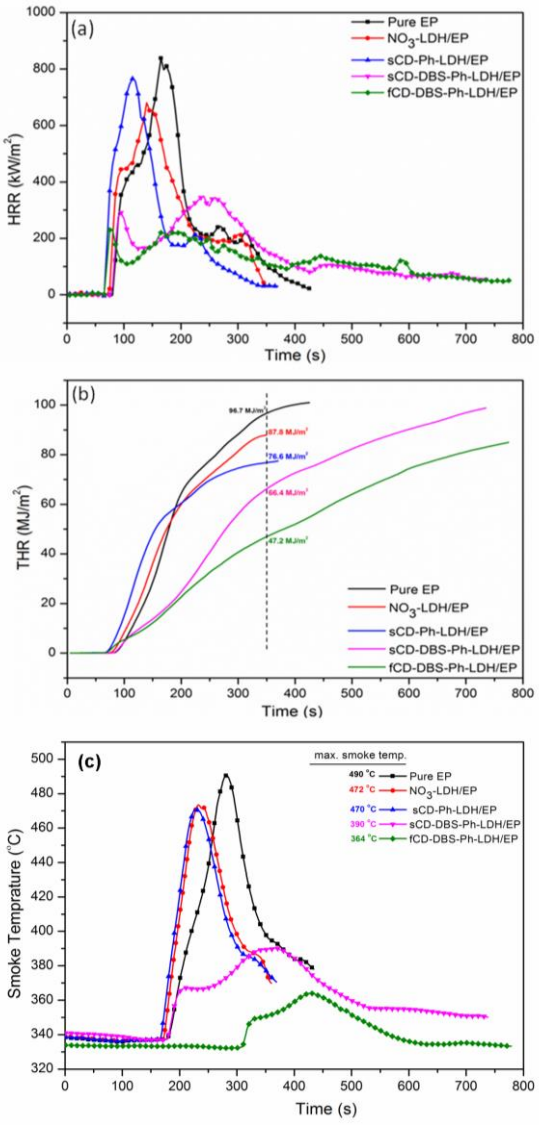

Fig. 6 (a) Heat release rate, (b) total heat release and (c) smoke temperature versus time curves of epoxy and its nanocomposites from cone calorimeter tests.

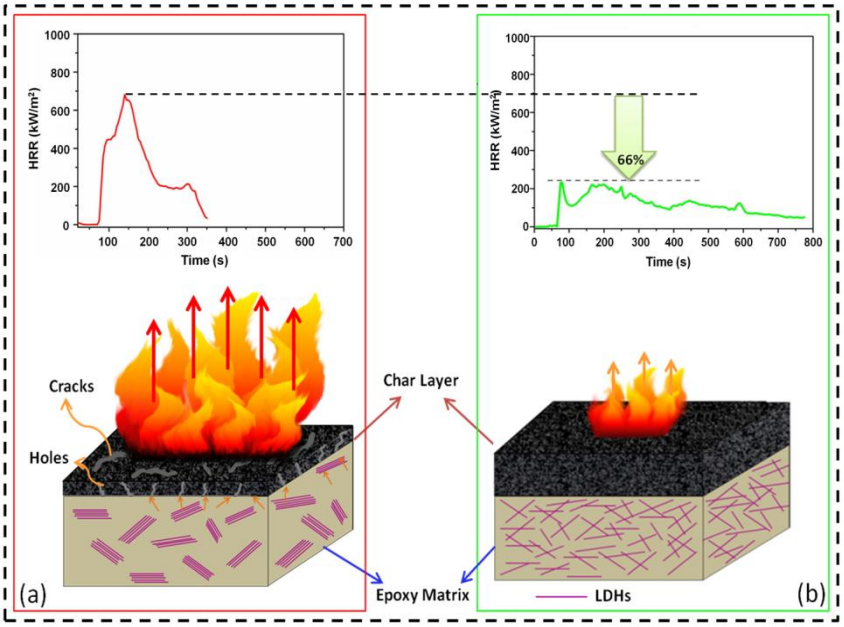

Fig. 7 Schematic illustration of the barrier effect of the (a) NO_3-LDH/EP and (b) fCD-DBS-Ph-LDH/EP.

epoxy nanocomposites was probably due to the reduced amount of epoxy converted into organic volatiles, since the organic volatiles are the major source of smoke particles.[30]

Based on the cone calorimeter results, the fCD-DBS-Ph-LDH/EP indicating a condensed phase mechanism, as shown in Fig. 7, hence showed significantly lower mass loss and higher char yield compared to other samples. The higher char yield resulted in quenching the flame which means less epoxy converted into flammable gases. Formation of a thick char layer was on the surface of the matrix served as a thermal insulating barrier to separate oxygen from burning materials and also, prevent combustible gases from feeding the flame zone, as shown in Fig. 7b. This was the reason for the reduced heat release rate and total heat release of fCD-DBS-Ph-LDH/EP composite in the cone calorimeter test.

More investigation achieved by study the morphology of the char residues of the samples after cone calorimeter test by SEM. As shown in Fig. 8a, b and c, the char residues of NO_3-LDH/EP, sCD-Ph-LDH/EP and sCD-DBS-Ph-LDH/EP showed a cracked, fluffy and full of open wholes toward the surface of the char layer, while fCD-DBS-Ph-LDH/EP (Fig. 8d) displayed a consolidated wafer structure in the cross-section and thick and continues char layer which resulted in significant reduction of heat and mass transfer and thus significantly enhanced the flame retardancy.

Table 3 Combustion parameters obtained from cone calorimeter

Sample	TTI (s)	pHRR (kW/m^2)	TSP (m^2)	Ave. HRR in 300 s	Char residue (%)
Pure EP	76±3	837±12	61.9±0.7	330±7	14±0.7
NO_3- LDH/EP	75±2	679±19	52.0±1.2	360±11	20±1.3
sCD-Ph-LDH/EP	66±2	762±26	37.2±1.3	256±19	16±1.2
sCD-DBS-Ph-LDH/EP	78±3	390±21	36.2±0.8	234±13	25±1.9
fCD-DBS-Ph-LDH/EP	69±2	232±18	22.5±1.2	162±12	27±1.4

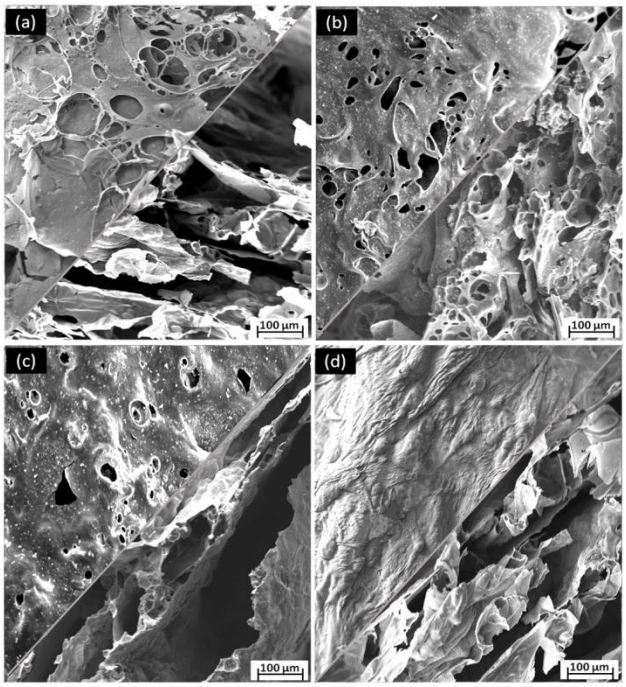

Fig. 8 SEM images of the surface and cross-section of the residual chars of (a) NO_3-LDH/EP, (b) sCD-Ph-LDH/EP, (c) sCD-DBS-Ph-LDH/EP and (d) fCD-DBS-Ph-LDH/EP after the cone calorimeter test.

3.7. Anti-UV properties

Since the presence of Chalcone (-CO-CH=CH-) units are capable of absorbing UV energy and release of energy into the environment as thermal energy, resulting in increasing the

photo-stability of the polymers as a UV absorber through formation of isomers,[27] we expect such anti-UV function impart to epoxy resin by forming the proposed polymer nanocomposites in this study if the multifunctional LDHs work like nanocarrier.

3.7.1. Impact properties after UV irradiation

Impact results of non-exposed and ultraviolet (UV) exposed pure EP and its nanocomposites are presented in Fig. 9. For the non-exposed samples, it was indicated that the addition of NO_3-LDH resulted in decreasing the impact strength of the nanocomposite compared to those of pure EP. Poor interfacial interaction between fillers and epoxy matrix was attributed to the large agglomerations of NO_3-LDH which is observed in the TEM images of NO_3-LDH/EP. In contrast, fCD-DBS-Ph-LDH/EP showed better impact strength as compare to the NO_3-LDH/EP and sCD-DBS-Ph-LDH/EP. With the increase of UV irradiation time, the impact strength gradually decreased. It is observed that 400 h UV radiation had very significant deteriorative effect on the impact strength of the pure EP (-40%), NO_3-LDH/EP (-25%), and sCD-DBS-Ph-LDH/EP (-37%). In contrast to NO_3-LDH/EP, Chalcone/EP showed much lower reduction (-15%) in the impact strength by increasing the time of exposure to 400 h, suggesting that chalcone was the main contributor to the anti-UV property. The addition of chalcone species can effectively protect the macromolecular networks from decomposition by UV irradiation, and the maintenance of the integrity of the macromolecular networks is responsible for the improved impact strength of fCD-DBS-Ph-LDH/EP. After exposure to UV irradiation for 400 h, fCD-DBS-Ph-LDH/EP showed further reduction (-13%) in the impact strength, indicating the good UV protection effect of chalcone-CD complex.

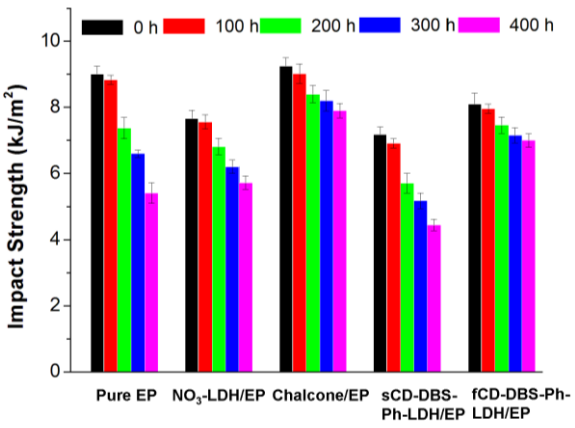

Fig. 9 Impact behaviour of pure EP and epoxy composites before and after UV exposure.

3.7.2. Micro-indentation test after UV exposure

Micro-indentation was used to determine the series of material properties across the interface from the UV exposed surface to the bulk material.[24] Fig. 10 illustrates typical indentation loading and unloading curves for pure epoxy and epoxy nanocomposites upon exposing time, indicating similar behaviors between the neat epoxy and nanocomposite. Figure 11 presents the displacement profiles plotted as a function the distance from the specimen surface. The change in displacement was a reflection of the diffusion process of free radicals and oxygen causing the degradation from the exposed surface into the depth of materials. With an increased exposure time, the effect was felt deeper in the material, which suggested a thicker degraded layer for a longer exposure time. When comparing the displacement profiles for the neat epoxy and the nanocomposite, their degradation behaviors and mechanical responses were very different. The displacement profile increased gradually from the surface and deeper into the material for neat epoxy, NO_3-LDH/EP and sCD-

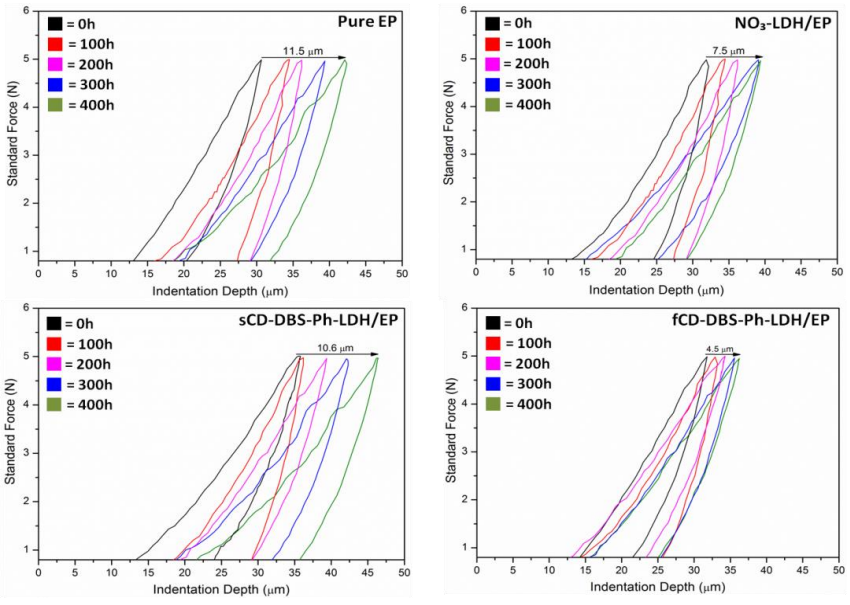

Fig. 10 Micro indentation of pure EP and epoxy nanocomposites before and after UV radiation.

Journal Name

ARTICLE

DBS-Ph-LDH/EP whereas, the profile dropped very rapidly and reached a steady state at much shallower depth for the fCD-DBS-Ph-LDH/EP nanocomposite which functionalized by chalcone. This may explain how the diffusion process of free radicals and oxygen and the associated degradation were delayed by the nanocomposite functionalized by chalcone.

The synergistic effect of the chalcone and exfoliated layers of LDH with a high aspect ratio served as barrier walls to restrict the movements and interactions between the species causing photo-degradation within the confined free volumes between the polymer molecules.[25] It can be concluded that the degraded thickness gradually increased with exposure time for pure EP, NO_3-LDH/EP and sCD-DBS-Ph-LDH/EP without UV barrier, and it was consistently smaller for the functionalized nanocomposite with UV barrier. The comparison confirmed the ameliorating effect of chalcone against the deterioration caused by photo-degradation.

Fig. 11 shows optical micrographs of the specimens before and after being subjected to the UV exposure. As it can be observed from the images of pure EP, NO_3-LDH/EP and sCD-DBS-Ph-LDH/EP, revealed the formation of inflammation and micro-cracks in the surface of the epoxy matrix. This phenomenon was induced by the polymer matrix becoming excessively brittle due to increased cross-linking resulting from photo-oxidation reactions caused by UV radiation. In contrast, 400h of UV exposure did not result in any significant changes in morphology of fCD-DBS-Ph-LDH/EP sample.

3.7.3. Three Point Flexural test after UV irradiation

Stiffness versus time results of pure EP and its LDH composites are presented in Fig. 12. Pure epoxy exhibited a steep decrease in the stiffness with increasing the exposure time. In contrast to pure epoxy, NO_3-LDH/EP showed more reduced trend in the stiffness as the UV exposure time increases, indicating the poor UV resistance. In the case of the sCD-DBS-Ph-LDH/EP composite, the stiffness also decreased with the increase of the UV exposure time. As for the fCD-DBS-Ph-LDH/EP nanocomposite, the stiffness was reduced slowly after UV irradiation which was indicated the diffusion of the UV radiation significantly decreased due to the UV absorption effect of chalcone species while the LDH layers served as physical barrier for shielding the underlying matrix from UV irradiation.

4. Conclusions

To conclude, we developed functionalized LDHs via multifunctional intercalation and the crucial step was to design the modifiers. In this paper, hydroxypropyl-sulfobutyl-beta-cyclodextrin equipped with chalcone specie, SDBS and phytic acid were designed as co-modifiers. A striking phenomenon was observed: with only 7 wt% of fCD-DBS-Ph-LDH, the resultant epoxy nanocomposite passed UL-94 V0 rating and significant reduction in the pHRR (-72 %) was achieved in the cone calorimeter test compared to the pure epoxy.

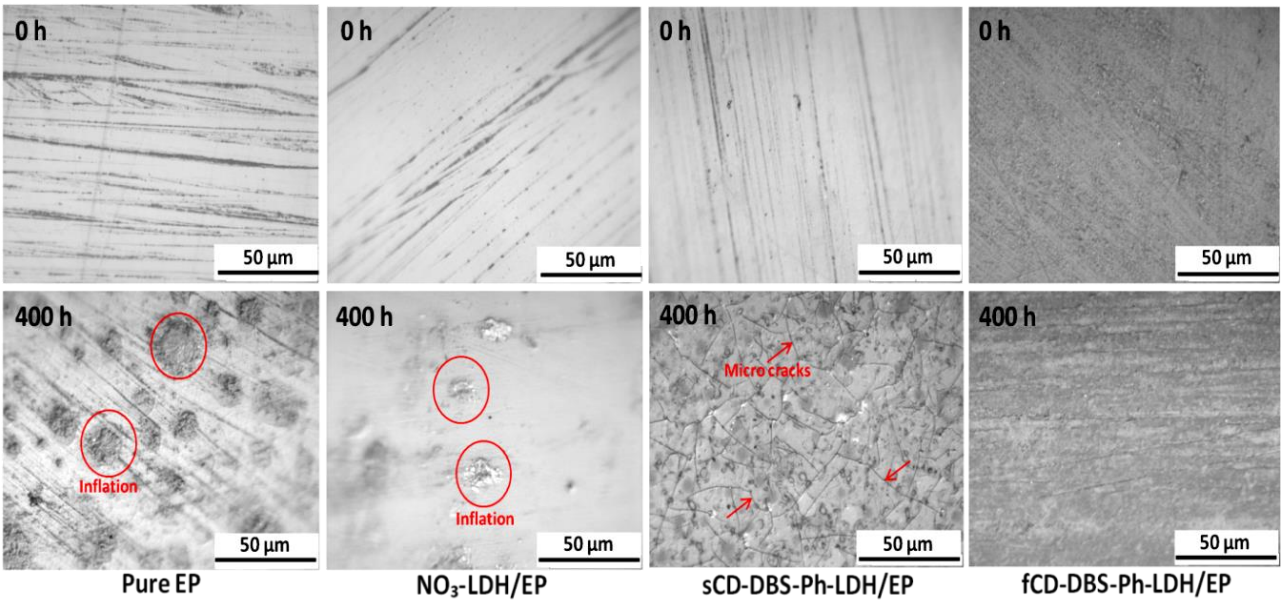

Fig. 11 Optical microscope images of the pure EP and epoxy nanocomposites before and after the UV exposure.

Journal Name

ARTICLE

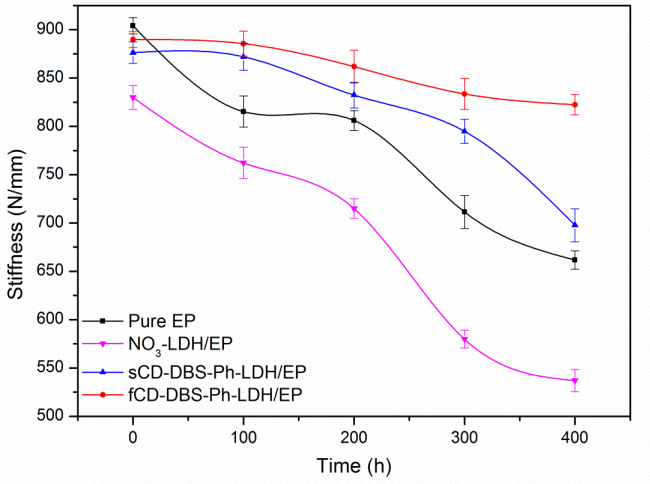

Fig. 12 Stiffness versus UV radiation time plots for pure EP and its nanocomposites.

Furthermore, fCD-SDBS-Ph-LDH/EP nanocomposite exhibited excellent anti-UV properties in terms of high preservation on impact, flexural and micro-mechanical properties after 100, 200, 300 400h UV irradiation, respectively, owing to the presence of chalcone specie that served as UV absorber. This multi-modifiers' nano-hybrid material developed in this work will offer a promising solution for developing multifunctional high performance polymer nanocomposite.

Acknowledgements

This research is funded by the European Commission under the 7th Framework Programme (Marie Curie Career Integration Grant, GA-321951) and Spanish Ministry of Economy and Competitiveness (MINECO) under Ramón y Cajal fellowship (RYC-2012-10737). Also, the authors are grateful to the nice discussion and comments from Prof. Francisco J. Velasco Lopez.

Notes and references

1 R. Jeng, S. Shau, J. Lin, W. C. Su and Y. S. Chiu, *Eur. Polym. J.*, **2002**, *38*, 683-693.
2 C. S. Wang and J. Y. Shieh, *Eur. Polym. J.*, **2000**, *36*, 443-452.
3 H. J. Sue, K. T. Gam, N. Bestaoui, N. Spurr and A. Clearfield, *Chem. Mater.*, **2004**, *16*, 242-249.
4 D. Sun, C. Chu and H. Sue, *Chem. Mater.*, **2010**, *22*, 3773-3778.
5 B. K. Kandola, A. R. Horrocks, P. Myler and D. Blair, *J. Appl. Polym. Sci.*, **2003**, *88*, 2511-2521.
6 C. H. Lin, T. Y. Hwang, Y. R. Taso and T. L. Lin, *Macromol. Chem. Phys.*, **2007**, *208*, 2628-2641.
7 S. D. Shaw, A. Blum, R. Weber, K. Kannan, D. Rich, D. Luca, C. P. Koshland, D. Dobraca, S. Hanson and L. S. Birnbaum, *Organohalogen Compd.*, **2011**, *73*, 2036-2039.
8 S. Bourbigot, S. Duquesne, G. Fontaine, T. Turf and S. Bellayer, *Mol. Cryst. Liq. Cryst. Sci.*, **2008**, *486*, 325-339.
9 E. Kalali, X. Wang and D. Y. Wang, *J. Mater. Chem. A*, **2015**, *3*, 6819-6826.
10 C. Li, J. T. Wan. E. Kalali. H. Fan and D. Y. Wang, *J. Mater. Chem. A*, **2015**, *3*, 3471-3479.
11 S. Ma, C. Fan, L. Du, G. Huang, X. Yang, W. Tang, Y. Makita and K. Ooi, *Chem. Mater.*, **2009**, *21*, 3602-3610.
12 D. Y. Wang, A. Das, A. Leuteritz, R. N. Mahaling, D. Jehnichen, U. Wagenknecht and G. Heinrich, *RSC Adv.*, **2012**, *2*, 3927-3933.
13 B. Zumreoglu-Karan and A. Nedim Ay, *Chem. Pap.* **2012**, *66*, 1-10.
14 N. J. Kang, D.Y. Wang, B. Kutlu, P. C. Zhao, A. Leuteritz, U. Wagenknecht and G. Heinrich, *ACS Appl. Mater. Inter.*, **2013**, *5*, 8991-8997.
15 Z. Matusinovic and C. A. Wilkie, *J. Mater. Chem.*, **2012**, *22*, 18701-18704.
16 Y. Gao, J. Wu, Q. Wang, C. A. Wilkie and D. T. O'Hare, *J. Mater. Chem. A*, **2014**, *2*, 10996-11016.
17 C. Manzi-Nshuti, P. Songtipya, E. Manias, M. Jimenez-Gasco and J. Hossenlopp, *Polymer*, **2009**, *50*, 3564-3574
18 N. Nhlapo, T. Motumi, E. Landman, S. M. C. Verryn and W. W. J. Focke, *J. Mater. Sci.*, **2008**, *43*, 1033-1043.
19 N. Iyi, Y. Ebina and T. J. Sasaki, *J. Mater. Chem.*, **2011**, *21*, 8085-8095.
20 H. Zhang, Z. P. Xu, G. Q. Lu and S. C. Smith, *J. Phys. Chem. C*, **2009**, *113*, 559-566.
21 G. R. Williams, N. H. Rees and D. T. O'Hare, *Solid State Sci.*, **2009**, *11*, 1229-1238.
22 X. Wang, E. Kalali and D. Y. Wang, *ACS Sustainable Chem. Eng.*, **2015**, *3*, 3281-3290.
23 J. Akhavan, E. Koh, S. Waring and E. Kronfli, *Polymer*, **2001**, *42*, 7711-7718.
24 R. S. C. Woo, H. Zhu, C. K. Y. Leung and J. Kim, *Compos. Sci. Technol.*, **2008**, *68*, 2149-2155.
25 B. G. Kumar, R. P. Singh and T. Nakamura, *J. Compos. Mater.*, **2002**, *24*, 2713-2721.
26 Z. K. Si, Q. Zhang, M. Z. Xue, Q. R. Sheng and Y. G. Liu, *Res. Chem. Intermed.*, **2011**, *37*, 635-646.
27 D. H. Choi, S. J. Oh, H. B. Cha and J. Y. Lee, *Eur. Polym. J.*, **2001**, *37*, 1951-1959.
28 Y. Ren, X.Q. Ma, S.Q. Yu and X.D. Sun, **2012**, US8278437.
29 D. Y. Wang, F. Costa, A. Vyalikh, A. Leuteritz, U. Scheler, D. Jehnichen, U. Wagenknecht, L. Häußler and G. Heinrich, *Chem. Mater.*, **2009**, *21*, 4490-4497.
30 X. Wang, W. Y. Xing, X. M. Feng, B. Yu, H. D. Lu, L. Song and Y. Hu, *Chem. Eng. J.*, **2014**, *250*, 214-221.